Journal of Techniques, ISSN: 2708-8383, Vol. 8, No. 2, 2026, Pages 71-80
https://doi.org/10.51173/jt.v8i2.2896

JOURNAL OF TECHNIQUES

Journal homepage: http://journal.mtu.edu.iq

RESEARCH ARTICLE - ENGINEERING (MISCELLANEOUS)

A Dual Band Substrate Integrated Waveguide Antenna with DRA for 5G Mobile Application

Agilesh Saravanan Ramamoorthi[1], Bendalam Alekhya[2], Ch Amarnatha Sarma[3], Sudha Rani V[4], Yalavarthi Usha Devi[1*], Boddapati T P Madhav[1]

[1]Antennas and Liquid Crystals Research Center, Koneru Lakshmaiah Education Foundation, Guntur, Andhra Pradesh-522302, India

[2]Department of Electronics and Communication Engineering, Vallurupalli Nageswar Rao Vignana Jyothi Institute of Engineering and Technology (VNRVJIET), Hyderabad-500090, India

[3]ECE Department, Geethanjali Institute of Science & Technology, Nellore, India

[4]School of CS&AI, SR University, Warangal, Telangana, India

[*] Corresponding author E-mail: ushadevi.yalavarthi@gmail.com

Article Info.

Article history:

Received
25 February 2026

Revised
04 June 2026

Accepted
16 June 2026

Published
30 June 2026

Abstract

This paper describes the design, evaluation, and investigational validation of a dual-band Substrate Integrated Waveguide (SIW) supported Dielectric Resonator Antenna (DRA) for fifth-generation (5G) applications. The designed antenna is realized on a Rogers RT/duroid 5880 substrate ($\varepsilon r = 2.2$, $\tan\delta = 0.003$, thickness = 1.2 mm) and excited by a microstrip-fed SIW structure. A cubic Dielectric Resonator (DR) with dimensions of 5.2 × 5.2 × 5.2 mm³ and dielectric constant of 9.9 is positioned over a modified H-shaped slot engraved on the SIW cavity. The proposed modified-H-shaped slot serves as a magnetic-coupling aperture, enabling controlled excitation of multiple resonant modes and facilitating dual-band operation at 28 GHz/38 GHz in the Ka band. The designed antenna achieves a measured impedance bandwidth of 12.12% (26.02–30.26 GHz), a realized gain of 7.1 dBi, and a radiation efficiency of 84.2% at 28 GHz. When operated at 38 GHz, it displays a bandwidth of 8.95% (37.01–40.07 GHz), a maximum gain of 7.28 dBi, and a radiation efficiency of 81.9%. Moreover, the proposed antenna exhibits circular polarization with an axial ratio below 3 dB at both operating frequencies, enabled by the combined contributions of the altered H-slot and the dielectric resonator. The antenna is constructed and optimized using a full-wave electromagnetic simulator (CST Microwave Studio), and its performance is well-matched between simulation and measurement results. The new SIW-DRA structure is seen to improve several parameters as compared to the SIW slot antennas.

Publisher: Middle Technical University

Keywords: Dual Band; Dielectric Resonator; Mobile Applications, 5G; Substrate Integrated Waveguide.

1. Introduction

In the modern age of wireless communications, there is a need for small, multi-band, highly efficient antennas that support advanced applications such as 5G systems [1, 2]. SIW is a potential solution due to its low transmission loss, high quality factor, and manufacturability using common printed circuit board (PCB) techniques [3, 4]. SIW can be considered a planar structure mimicking a common waveguide, making it very useful for millimeter-wave applications. Many SIW structures, including dumbbell-slot SIWs, L-shaped-slot SIWs, and multiple-cut SIWs, have been reported for the design of wideband or multiband antennas [5–7]. Dielectric Resonator Antennas (DRAs) are very popular among many designers because of their high radiation efficiency, tunable design parameters, and operation with minimal conductor losses at higher frequencies [8]. Many researchers have studied hybrid SIW-DRA antennas to improve the bandwidth and radiation features [9–12]. The hybrid SIW-DRA offers the benefits of both SIW and DRA, i.e., efficient energy confinement in SIW and improved radiation properties in DRA. On the other side, though there have been many designs with SIW-DRA structures, many drawbacks remain in these designs, namely:

(i) lack of control over the dual bands' excitation, (ii) poor electromagnetic coupling between the SIW cavity and the radiator at millimeter-wave frequencies, and (iii) lack of polarization diversity, in particular circular polarization. Furthermore, many antennas that claim dual-band properties exhibit either narrow impedance bandwidths or poor gain at high frequencies, limiting their usefulness in the new 5G millimeter-wave regime. The need for better antenna designs becomes evident from this problem.

Nomenclature and Symbols			
SIW	Substrate Integrated Waveguide	DRA	Dielectric Resonator Antenna
5G	Fifth-Generation	DR	Dielectric Resonator
PCB	Printed Circuit Board	HL	Length
HW	Width	S1	Spacing
DWM	Dielectric Waveguide Model	AR	Axial Ratio

The objective of this study is to introduce an advanced SIW-DRA structure that can operate reliably in the dual band while maintaining good coupling, bandwidth, and circular polarization. However, the SIW-based slots developed to date exhibit problems, such as inadequate dual-band excitation and poor coupling between the SIW and the radiating antenna. To overcome the above drawbacks, this study proposes integrating an optimized SIW-DRA antenna system with a modified H-shaped slot. This novel system is based on the following innovative ideas. First, the modified H slot is designed to enhance magnetic currents within the SIW cavity and improve mode excitation. Unlike conventional slot geometries, this modification provides improved impedance matching and controlled dual-band resonance at 28 GHz and 38 GHz. Second, optimized integration of SIW and DRA enables efficient electromagnetic coupling, with the SIW cavity providing low-loss energy confinement and the DRA providing high radiation efficiency. This combined mechanism results in simultaneous improvement in bandwidth, gain, and circular polarization performance, which is not achieved in conventional SIW or DRA-based designs individually.

As a result, the proposed antenna achieves efficient dual-band operation in the Ka-band, with better performance than conventional SIW slot antennas. The combination of a modified slot design and optimized SIW–DRA integration makes the proposed antenna highly suitable for high-frequency 5G systems. Further section of this paper is arranged as follows: Section 2 illustrates antenna design methodology, Section 3 presents results and discussion, and Section 4 concludes the work.

2. Development of the Design

Figs. 1 and 2 show the geometry and reflection coefficient features of the designed SIW antenna with modified via structures. The SIW cavity is created due to the termination of the structure using equally spaced vias, where the vias represent the boundaries of the waveguide. Fig. 2(a) shows the reflection coefficient of the suggested antenna with and without a dielectric resonator antenna (DRA). Reflection coefficient values are named SIW_DRA_ALL-Without DRA and SIW_DRA_ALL-With DRA. As shown in Fig. 2, the addition of DRA greatly enhances impedance matching at 28/38 GHz.

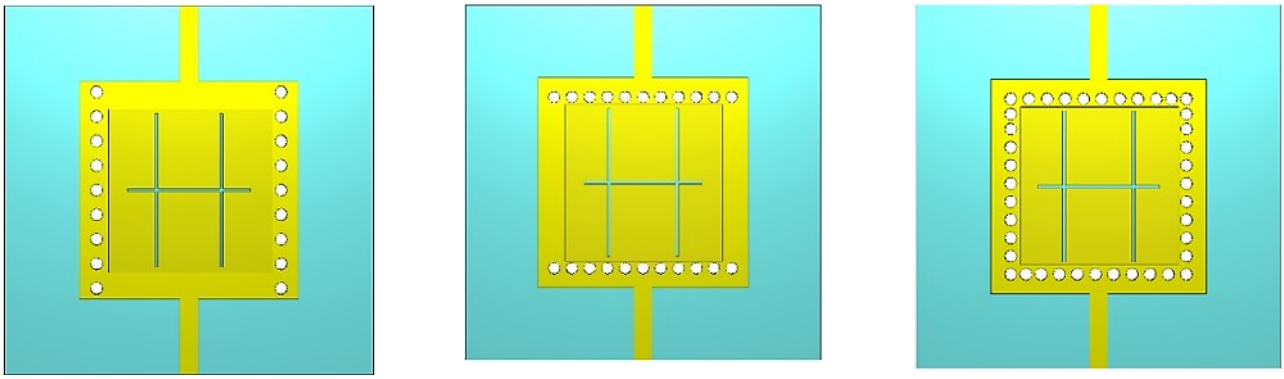

a) b) c)

Fig. 1. Geometric view of H-Slot antenna in top view; a) with vertical SIW(SIW_DRA_V), b) with horizontal SIW(SIW_DRA_H), and c) with all sided SIW(SIW_DRA_ALL)

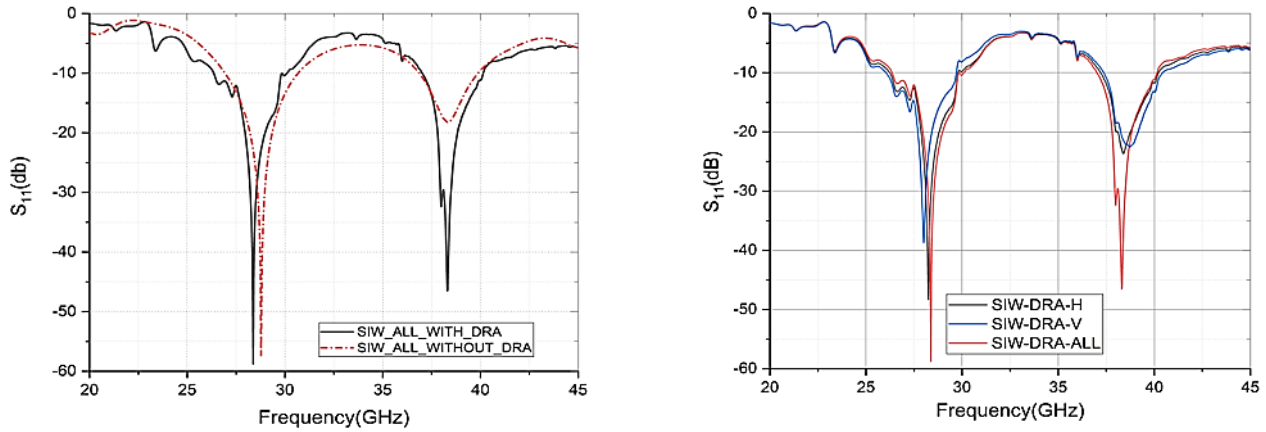

a) b)

Fig. 2. Evaluation of S_{11} reflection coefficient for; a) antenna with DRA and without DRA, and b) proposed antennas with modified SIW configuration with DRA

Fig. 2(b) shows how changing the via alignment affects the reflection coefficient. The modified H-slot, defined by its length (HL), width (HW), and spacing (S1), is the main factor in controlling the electromagnetic response. It acts like an equivalent magnetic current source, disturbs the surface current, and allows electromagnetic energy to escape from the SIW cavity. At 28 GHz, there is a big drop in return loss, but at 38 GHz, the improvement is modest. This shows that a regular H-slot won't cut it if you want solid dual-band performance. To solve this, a dielectric resonator antenna (DRA) is added to the center of the SIW cavity using vertical via alignment, as shown in the SIW_DRA_V setup (Fig. 1(a)). Here, electromagnetic energy moves from the SIW's cavity to the DRA's through the H-slot. The H-slot acts as a magnetic current source, exciting the DRA and boosting bandwidth, gain, and radiation efficiency. The interaction between cavity fields and the dielectric resonator gives rise to multiple resonant modes, resulting in dual-band operation at 28 GHz/38 GHz, as shown in Fig. 2(b).

With the horizontal via alignment (SIW_DRA_H, Fig. 1(b)), the modified H-slot still alters the surface current distribution and improves radiation, but it does not yield optimal results. It achieves good impedance matching at 28 GHz, but the coupling at 38 GHz remains weak; it just doesn't pull enough energy from the SIW cavity into the DRA at those higher frequencies. Now, the proposed setup (SIW_DRA_ALL, Fig. 1(c)) takes it a step further. It uses optimized placement on all sides and carefully positions both the DRA and the H-slot. This significantly increases electromagnetic coupling, providing a better impedance bandwidth across both bands. Additionally, by offsetting the DRA relative to the H-slot, the coupling becomes even stronger, improving resonance at 38 GHz and maintaining stable dual-band operation. At Fig. 2(a), the comparison makes it clear: The SIW–DRA configuration beats the traditional H-slot SIW antenna across the board. Energy transfer from the SIW cavity to the DRA through the new H-slot results in better impedance matching, a lower reflection coefficient, and a wider bandwidth at both frequencies.

3. Factors in Antenna Geometry and Layout

The 3D model of the designed Dual Port SIW antenna with DRA is provided in Fig. 3(a). This particular antenna is designed on the Rogers RT/duroid 5880 substrate, with a relative permittivity (ε_r) of 2.2, loss tangent (tan δ) of 0.003, and a thickness of 1.2 mm. A 0.035 mm-thick copper sheet is used on both sides of the substrate, as illustrated in Fig. 3(b and c).

For the proposed design, the antenna's input impedance is kept at 50 Ω and excited via a microstrip line. The parameters for the dielectric resonator used here are: dimension 5.2 × 5.2 × 5.2 mm³, dielectric constant 9.9, and loss tangent 0.0009.

The resonant frequencies (f_0) at 28 GHz and 38 GHz are calculated using the Dielectric Waveguide Model (DWM). The formula is based on Eqs. 1 to 4, as described in [8]. Here, D_x, D_y, and D_z are wave numbers along the x, y, and z axes, respectively, and D_0 is the wave number in free space related to the resonant frequency. Here, c represents the velocity of light in free space, and εr is the relative permittivity of the dielectric resonator.

$$f_0 = \frac{c}{2\pi\sqrt{\varepsilon_x}} \sqrt{D_x^2 + D_y^2 + D_z^2} \quad (1)$$

$$D_x = \frac{\pi}{x1} \quad (2)$$

$$D_z = \frac{\pi}{z1} \quad (3)$$

$$Dy \tan\left(\frac{Dyy1}{2}\right) = \sqrt{(\varepsilon_x - 1)D_0^2 - D_y^2} \quad (4)$$

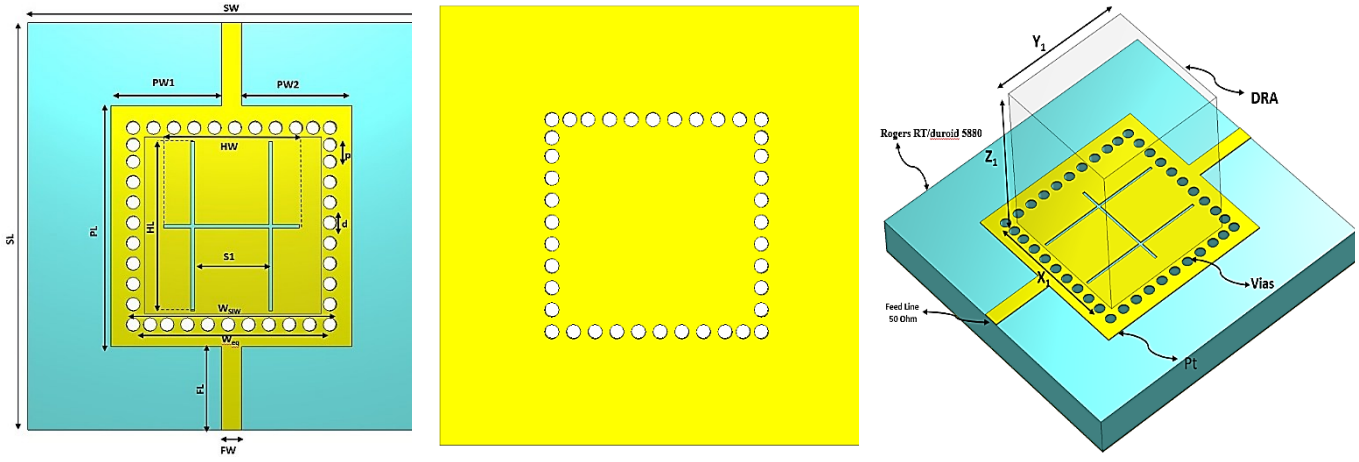

a) b) c)

Fig. 3. Structure of the projected antenna; a) Top view, b) Bottom view, and c) 3D view

The H-shaped cut configuration in the top wall of the SIW effectively excites its corresponding mode. This mode is characterized by a complete ground located at the bottom of the substrate. The effective width of a waveguide, denoted as Weq, is determined by applying Eqs. 5 and 6 [13, 14] to a conventional waveguide known as WR 430:

$$w_d = \frac{w}{\sqrt{\varepsilon_r}} \quad (5)$$

$$w_{eq} = w_d + \frac{d^2}{0.95p} \quad (6)$$

The variables in this context are described as follows: w represents the thickness of the conservative air waveguide, wd represents the thickness of the dielectric waveguide, εr represents the substrate permittivity, d denotes the via diameter, and p represents the distance among the vias.

On behalf of the greater value of diameter d [14], the equation is invalid, therefore the below Eq. 7 is redefined by adding the d/W_{eq} ratio

$$W_{siw} = W_{eq} - 1.08\frac{d^2}{p} + 0.1\frac{d^2}{W_{eq}} \quad (7)$$

The purpose of metal via holes is to form a structured SIW. Structured SIW is composed of double rows of metallic vias with a diameter d and a spacing p between them. Diameter and spacing values of the via holes can be determined by using Eqs. 8-10 [15, 16], where minimizing energy leakage is considered:

$$d < \frac{\lambda_g}{5} \quad (8)$$

$$p \leq 2\,d \quad (9)$$

where the wavelength for guiding, λ_g, is

$$\lambda_g = \frac{2\pi}{\sqrt{\frac{(2\pi f)^2 \varepsilon_r}{c^2} - \left(\frac{\pi}{a}\right)^2}} \quad (10)$$

The following Eq. 11 [15] condition should be used to overcome any bandgap effects in the resonant bandwidth,

$$\frac{P}{\lambda_c} < 0.25 \quad (11)$$

The term λ_c represents the wavelength associated with the cutoff frequency of the waveguide. In the proposed SIW configuration, one of the ends of the structure is short-circuited to establish standing wave patterns within the waveguide cavity [12]. For efficient signal transfer, a tapered microstrip transition is incorporated to match the impedance between the 50 Ω microstrip feedline and the SIW structure. Preliminary measurements of taper, denoted by l_t and w_t, are estimated using the design equations reported in [17]. Following a comprehensive parametric optimization process, the final optimized geometrical parameters are summarized in Table 1.

This paper examines three distinct antenna arrangements for a dual-port SIW structure with a DRA to achieve resonance in both 28/38 GHz frequency bands. The aim is to provide coverage across the Ka-band, which is essential for advanced wireless systems, while ensuring compatibility with existing 4G bands.

Table 1. Proposed antenna DHF-DRA-V dimensions

Notation	Value (mm)	Notation	Value (mm)	Notation	Value (mm)	Notation	Value (mm)
SL	12	GL	12	Pt	0.035	PW1	3.25
SW	12	GW	12	St	1.2	PW2	3.25
FL	2.45	S1	2	X1	5.20	HW	5
FW	0.60	W_{eq}	5.60	Y1	5.20	HL	4
p	0.8	W_{SIW}	6	Z1	5.20	Ht	0.5
d	0.4	Gt	0.035	PL	7.10		

4. Parametric Analysis

The key design parameters of the proposed antenna affect its bandwidth response; this section explains how to find the optimal configuration, a detailed study of all the parameters is conducted. The width and length of the DRA, shown as x1 and y1 in Fig. 4(a and b), are very important for controlling the resonance frequency. As the width (x1) increases, the bandwidth changes significantly in the middle and upper frequency bands. This happens because, although the modified H-shaped slot is under the DRA element, the energy radiated is not well coupled to the SIW cavity at 28 GHz and 38 GHz. If the length, which is increasing, affects the width of the DRA in the direction of the feed. This decreases the resonance frequencies in both upper bands. The reason is that the wave number ky in the y direction decreases, so the resonance frequency decreases as well.

As seen in Fig. 4(c), as the height of the DRA z1 increases, the resonant frequencies at 28/38 GHz decrease towards lower values. This is because, as the height of the dielectric resonator increases along the z-axis, the wave number kz decreases in the same direction. This is why the resonant frequencies are smaller. The working principle of the suggested antenna is based on the TE_y mode of a dielectric resonator. In this case, the electric field travels along the y-axis. It varies along both the x- and the z-axes. This is why an increase in the z-axis dimension leads to changes in the field within the resonator. As z1 increases, the resonant cavity's dimensions increase.

The results also show that the spot of the DRA along the x-axis (x1) does not affect the reflection characteristics much. This is because the x direction does not affect the field distribution of the TEy mode. On the other hand, moving DRA along the y-axis (y1) has a significant effect on the reflection coefficient. This is because the y-direction is the same as the electric-field component. Any change in this direction alters the coupling between the microstrip-fed modified H-shaped slot and the dielectric resonator. The TEy mode is well excited at both 28 GHz and 38 GHz when the DRA is in this position. This position is near the high-field region of the slot aperture. The best position is when x1 = 5.2mm, y1 = 5.2mm, and z1 = 6.4mm. At this position, the DRA is close to the microstrip transition. This better coupling improves impedance matching

and ensures stable dual-band operation. The DRA position is significant because of its function in dual-band applications. The position y1 of the DRA component z1 is vital, as the antenna's function depends on it.

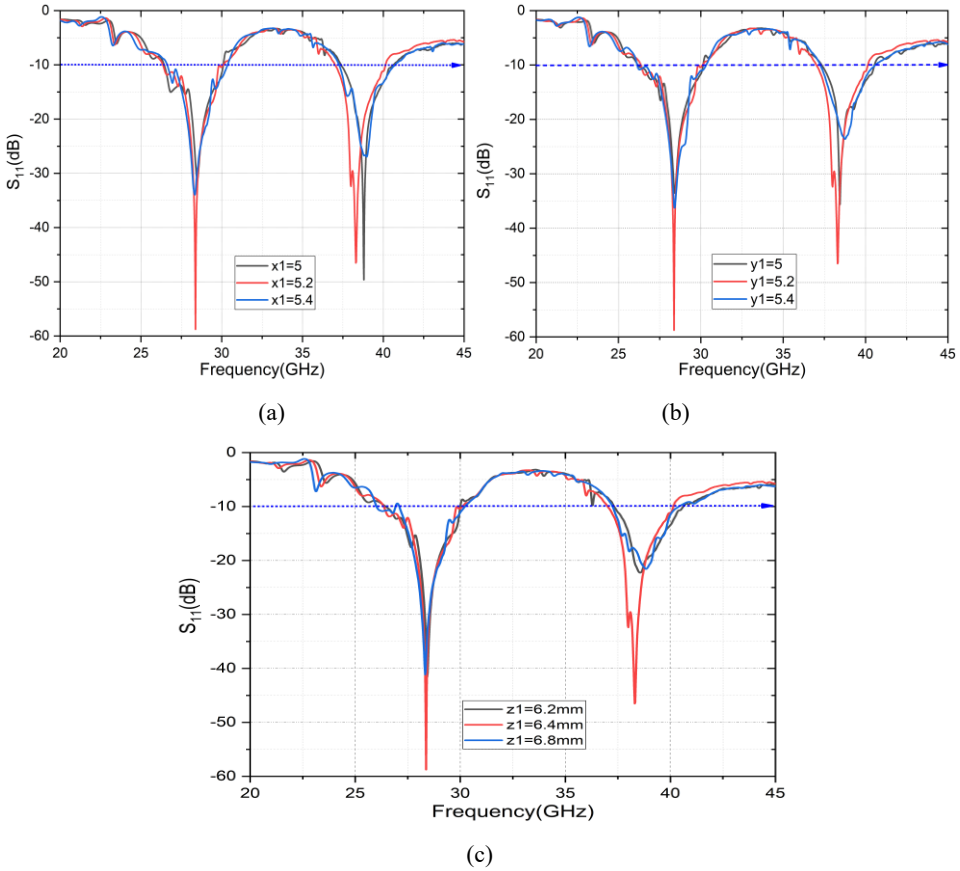

Fig. 4. Modeled $|S_{11}|$ for various DRA's parameters; (a) DRA length, (b) DRA width, (c) DRA height

5. Fabrication Results and Discussion

To achieve dual-band operation of the SIW-DRA at 28/38 GHz, the complementary nature of SIW and DRA is exploited, leveraging the benefits of both resonators. The SIW structure allows achieving good field confinement, low losses, and a high quality factor, while DRA offers high radiation efficiency and the possibility of exciting its modes. Thus, their integration provides improved impedance matching and stable radiation characteristics in millimetre-wave bands.

A modified H-shaped slot is used to provide a coupling element for connecting the SIW cavity to the DRA. Such a slot is responsible for controlling the excitation of the dominant TEy mode of the dielectric resonator. Magnetic coupling via an H-slot allows effective energy transfer from the microstrip line to the dielectric resonator. In contrast to traditional rectangular and circular slots, H-slots provide additional tuning options to enable dual-band operation of DRAs.

The behaviour at the two bands at 28/38 GHz mainly relies on the resonance behaviour of the proposed DRA and is predicted by the dielectric waveguide model (DWM). The resonant frequency as defined by this model primarily depends on the wave numbers (kx, ky, kz), which in turn depend on the resonator's size. This means that any change in x1, y1, and z1 results in a change in the wave number and, consequently, in the resonance behaviour.

5.1. Reflection coefficient and gain

Fig. 5(a) shows the dual-port SIW-DRA antenna prototype. The dual-port SIW-DRA antenna is fabricated using printed circuit board methods, and it has two feed ports as part of the SIW-DRA configuration. The base material is Rogers RT/duroid 5880, which has a permittivity (ε_r) of 2.2, and the ground planes and dual microstrip feed lines are cut from this material. The dielectric resonator is made from a material with permittivity (ε_r) of 9.9 and is shaped like a cube, placed over the SIW structure. The SIW sidewalls are made using metal-filled holes to ensure electromagnetic fields are contained and do not leak out.

The dual-port SIW-DRA antenna is attached to a vector network analyser via 50 Ω SMA connectors to measure signal scattering. The modelled and determined reflection coefficients, which are $|S_{11}|$ and $|S_{22},|$ match well. Show that the impedance is properly matched at both 28 GHz and 38 GHz. Also, the transmission coefficient $|S_{21}|$ is examined to see how well the ports are isolated from each other. The results show that $|S_{21}|$ is low, below −15 dB across the operating bands, indicating that the ports are well isolated. This isolation is mainly due to the SIW cavity structure, which confines the fields within the cavity and prevents direct coupling to the feed lines.

The way the fields are distributed in the TE mode of the DRA also helps reduce the extent of port-to-port interaction. The modified H-shaped slot also helps with isolation by keeping the coupling region small and stopping much energy from leaking between the two paths that excite

the antenna. As a result, each port can excite the DRA independently without interference from the other port. Overall, the simulated and measured values match closely, indicating that the anticipated dual-port SIW-DRA antenna design achieves impedance matching and high port isolation, making it suitable for dual-port and MIMO millimetre-wave applications. The dual-port SIW-DRA antenna works well for these applications.

(a) Prototype of dual-port SIW with a DRA (b) Measurement of the S parameter

Fig. 5. Assessment of the scattering parameter of the recommended antenna using the vector network analyzer

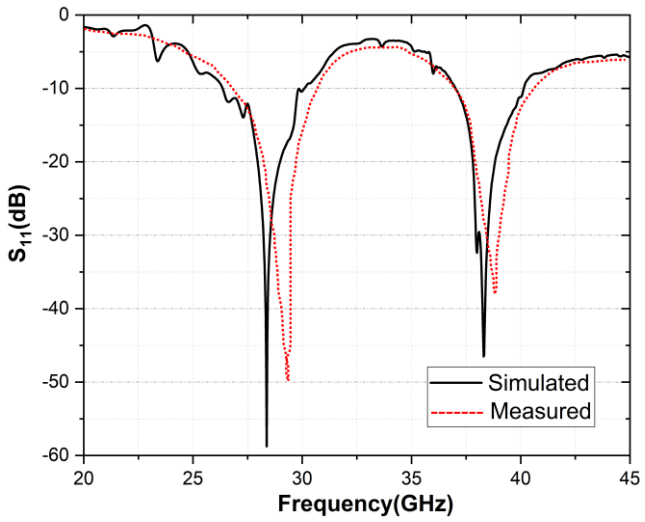

Fig. 6. Frequency response of measured return loss S_{11}

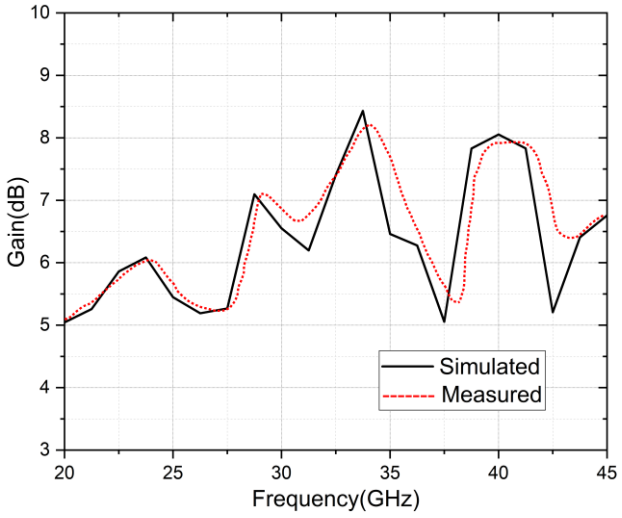

Fig. 7. Measured and simulated gain

The simulation and measurement of the reflection coefficient (|S11|) are compared according to the −10 dB impedance bandwidth criteria in Fig. 6. It is evident that the designed antenna performs well at two operating frequencies. At 28 GHz, the measured bandwidth is 15.06% (26.02–30.26 GHz), while the simulated bandwidth is 12.12% (27.28–30.50 GHz). At 38 GHz, the measured bandwidth is 7.93% (37.01-40.07 GHz), while the simulated bandwidth is 8.95% (37.03-40.5 GHz). There is a slight difference between the measurements and simulations, due to fabrication tolerances, the air gap between the DRA and the substrate, and the use of adhesive in attaching the DRA. This is due to a change in the effective permittivity of DRA, and thus, there are some variations in the measured results. All measurement and simulation results have been summarised in Table 2. In addition, there is a slight drop in the measurement gain, which may be due to connector losses, fabrication imperfections, and unaccounted-for dielectric losses.

Table 2. Comparison between simulated results and measured results of the proposed antenna at dual band

Antenna Parameters		28GHZ	38GHz
Covered Bandwidth %	Simulated	15.06	7.93
	Measured	12.12	8.95
Gain(dB)	Simulated	7.32	7.64
	Measured	7.1	7.28
S_{11}(dB)	Simulated	-58.75	-46.52
	Measured	-49.45	-38.32

The modelled and experimentally obtained gain responses for the suggested antenna are shown in Fig. 7. The measurement results follow the simulation trend, thereby validating near-optimal impedance matching at both ports. Radiation patterns for both 28 GHz / 38 GHz show the broadside radiation. This is due to the SIW cavity structure, in conjunction with the modified H-shaped slot, which determines the field distribution and the nature of radiation. The modified H-slot is responsible for exciting resonances at both frequencies and is used as a coupling aperture in our case study. This compact structure has achieved gains of 7.1 dBi at 28 GHz and 7.28 dBi at 38 GHz. The field distribution of the structure shows that the electric fields from the two ports are focused at the center of the H-slot. The lateral electric fields cancel each other out in the x–y axis. At 38 GHz, the DRA contribution becomes more dominant, leading to a more directive radiation pattern with a narrower beamwidth. This is due to stronger confinement and efficient excitation of the resonant mode within the dielectric resonator. As a result, higher directivity and improved gain are achieved at this frequency, with a narrower beamwidth than at 28 GHz.

5.2. Radiation pattern

Simulated and calculated radiation patterns of the projected SIW-DRA antenna at 28GHz and 38GHz for φ = 0° (E-plane) and φ = 90° (H-plane) are provided in Fig. 8. At the two operational frequencies, it can be seen that suggested antenna has a permanent broadside radiation and symmetry in radiation patterns showing that the excitation of the radiator is efficiently done in the two bands considered. At 28 GHz, the two radiation patterns have relatively broad beams. In the E-plane case, the centre lobe beam width is relatively broad, and the directivity is not very high due to the predominant contribution of the SIW cavity and the H-shaped slot used in the design. The electromagnetic fields in this case are relatively distributed, resulting in a larger HPBW. The radiation pattern of the H-plane is relatively smooth and wide because of a more uniformly distributed magnetic field and effective dual port excitation. The beam width and sidelobes are low at both planes. At 38 GHz, the beam widths are relatively narrow, and the directivity is higher than at 28 GHz.

The difference in radiation characteristics between the two frequencies is mainly due to the shift from slot- or SIW-dominated radiation at 28 GHz to DRA-dominated radiation at 38 GHz. The dielectric resonator exhibits better field confinement and more efficient mode excitation at higher frequencies, resulting in a more, resulting in focused radiation pattern. The antenna provides maximum realized gains of about 7.1 dBi at 28 GHz and 7.28 dBi at 38 GHz. The reduced beam width at 38 GHz confirms the DRA's improved directivity and efficient radiation.

Fig. 9 illustrates the axial ratio (AR) characteristics of the proposed SIW-DRA Antenna. For the 28 GHz band, the axial ratio is estimated to be between 1 dB and 2 dB over the frequency range 26.34 to 30.33 GHz, yielding an axial ratio bandwidth of 14.32%. Likewise, for the 38 GHz band, the axial ratio is kept at 1 dB to 2 dB over the frequency range 36.1 to 40.35 GHz, giving an axial ratio bandwidth of 11.18%. These Figures show that the proposed antenna meets the criterion of having AR less than 3 dB, thereby achieving CP over the two frequency bands.

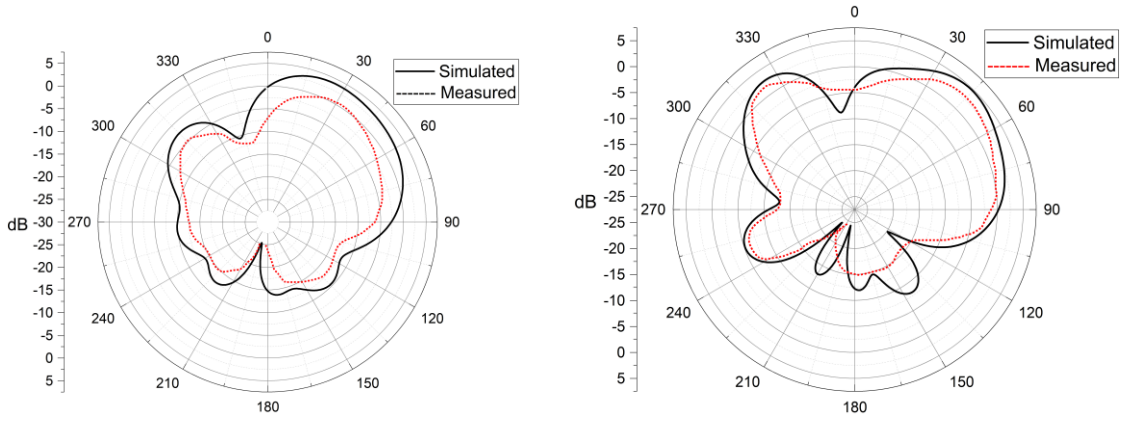

(a) (b)

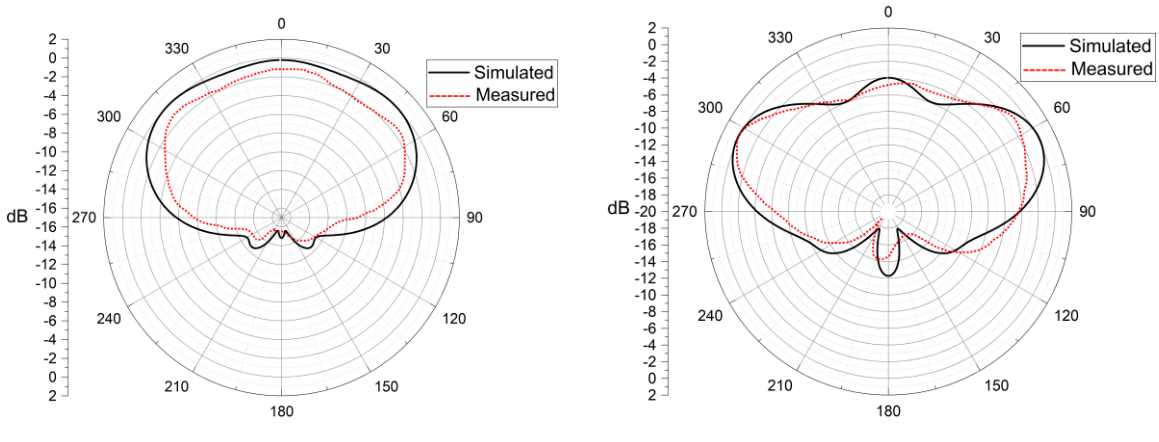

(c) (d)

Fig. 8. Radiation pattern comparison of measurement and simulation of the dual-port SIW with a DRA; (a) E-Plane at 28 GHz, (b) H-Plane at 28 GHz, (c) E-Plane at 38 GHz, and (d) H-Plane at 38 GHz

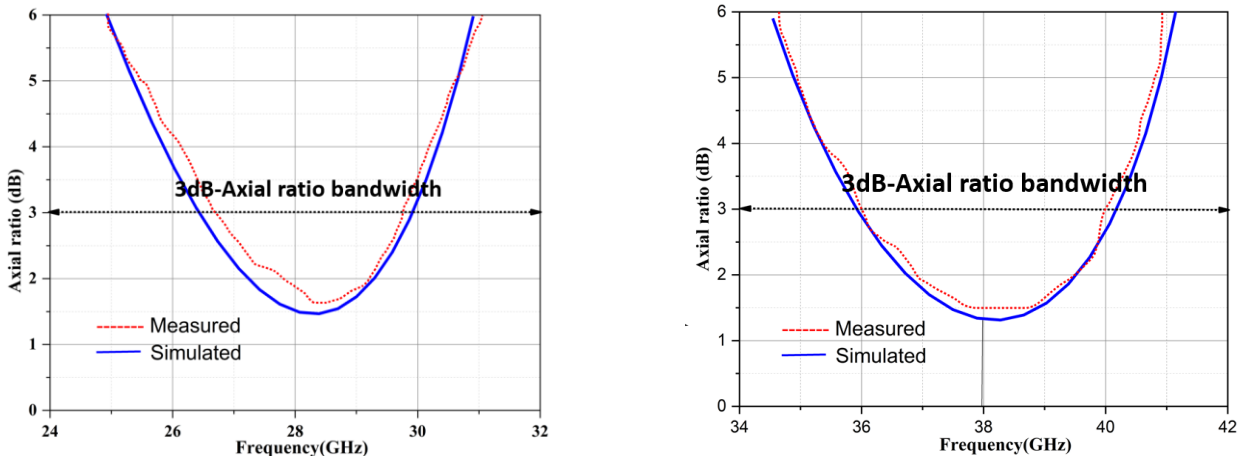

(a) (b)

Fig. 9. Simulation and measured axial ratio bandwidth in broadside direction; a)28GHz, and b)38 GHZ

The circular polarization behaviour of the proposed antenna is mainly due to the modified H-slot and the dielectric resonator antenna. The H-slot in the cavity is like a current source. It makes two resonant modes happen inside the antenna. These modes occur because the H-slot is asymmetrical. The length and width of the slot make these modes occur with significant strength, but with a phase difference of almost 90°. This phase difference is necessary for the antenna's circular polarization.

The DR is on top of the H-slot. It helps to make the modes balance each other. The electromagnetic connection between the cavity and the dielectric resonator antenna makes these modes stronger and more stable. The position and size of the dielectric resonator antenna are very important. They help to make the amplitude and phase of the modes just right. The circular polarization behaviour of the suggested antenna results from the combined effect of the modified H-slot and the dielectric resonator antenna. As a result, the interaction between the slot-induced magnetic currents and the DRA-supported resonant modes guided the creation of broadside circular polarization. This mechanism enables the antenna to maintain an axial ratio below 3 dB over both 28 GHz and 38 GHz bands, thereby confirming robust dual-band CP performance.

5.3. Performance analysis with published work

The proposed antenna is seen to offer significant advantages over earlier reported SIW-based slot antennas and SIW-DRA-based antenna structures. Compared with conventional slotted structures such as dumbbell, U-, or L-slot antennas (shown in Table 3) [18-28], the modified H-slot provides efficient excitation of dual resonant modes.

The proposed design achieves stable dual-band operation at millimeter-wave frequencies, unlike [20, 21], which mainly focus on broadband or single-band performance, making it more appropriate for 5G Ka-band applications. The proposed antenna exhibits improved impedance bandwidth and higher realized gain by optimizing the SIW-DRA coupling, compared to [23, 27], which achieve dual-band operation with narrow bandwidth or lower gain. Moreover, in comparison with the DRA-based designs discussed in [24-28], the novel antenna design exhibits bandwidths of 12.12% and 8.95%, gains of 7.1 dBi and 7.28 dBi, and radiation efficiencies of 84.2% and 81.9% at 28/38 GHz, respectively. Such enhancements are attributed to the following factors: (i) decrease in conductor and leakage losses because of the SIW configuration, (ii) high radiation efficiency associated with the DRA, and (iii) optimized size of the slots that guarantee proper impedance matching for both frequency ranges. Compared with slot antennas and similar designs, our proposed antenna performs well across two frequency bands. It has better gain stability and a wider bandwidth. Also, it is structurally simple and compact. However, the antenna's performance depends on the DRA's position and the H-slot's shape. This might make it hard to make many of these antennas that work the way they are supposed to. Overall, our antenna provides a good compromise between bandwidth, gain, efficiency, and simplicity. This makes it well-suited for 5G millimeter-wave applications.

Table 3. Comparison of the proposed antenna with another existing antenna

[Ref.]	Slot shape	DRA availability	Frequency (GHz)	Bandwidth(BW) (%)	Gain (dBi)	Total Antenna Efficiency (%)
[18]	Horizontal structured slot	No	2.6	16.05	5.1	92
[19]	Two vertical modeled cuts	No	3.6	12.61	Not stated	Not stated
[20]	Adumbbell-shaped slot	No	22	26.06	8	Not stated
[21]	U-shaped slot	No	28	13.79	7.2	Not stated
[22]	L-Structured slot	No	10.93 12.69	1.56 1.42	Not stated	Not stated
[23]	Two vertical cuts	No	28 38	1.61 5.82	5.2 5.9	Notstated
[24]	Horizontal cut	1RDRA	5.9	12.37	4.7	Not stated
[25]	plus-molded cut	1CDRA	6.56	8.54	3.7	Not stated
[26]	H-shaped slot	2RDRAs	60	10.03	5.5	81
[27]	Horizontal cut	1RDRA	28 38	13.62 9.94	Not stated	Not stated
[28]	U-shaped cut	1RDRA	1.8 2.6 3.7	19.5 6.58 8.21	4.9 4.4 6.7	81 72.7 73.5
Proposed Antenna	Modified H-Slot	1DRA	28 38	12.12 8.95	7.1 7.28	84.2 81.9

6. Conclusions

This paper reported the successful development of a dual-band SIW antenna with a DRA, which can be applied in future 5G communications. Specifically, the proposed antenna utilized a modified H-slot inside the SIW cavity, which changes the distribution of surface current and acts as a magnetic equivalent current source, thereby efficiently exciting the DRA. This enabled the antenna to operate in dual modes. The initial resonance frequency is 28 GHz, and its operation is attributed to the SIW cavity fundamental mode. In comparison, the high level of resonance around 38 GHz is attributed to a high-order mode due to the new arrangement of the slot and the loading of the field by the DRA, which reduces the effective electrical length. The effect of such a combination is stable dual-band operation without the addition of any further antennas for radiation. A continuation of this work could lead to expanding this concept to a multi-element antenna or a multiple-input multiple-output (MIMO) system, given its high efficiency and precise radiation.

Acknowledgements

The authors express their sincere gratitude for the funding provided by the DST-sponsored initiatives, File No. SR/FST/ET -I I/2019/450, and SR/PURSE/2023/196

References

[1] Aminu-Baba, M.; Rahim, M.K.A.; Zubir, F.; Iliyasu, A.Y.; Jahun, K.I.; Yusoff, M.F.M.; Gajibo, M.M.; Pramudita, A.A.; Lin, I.K.C. A compact triband miniaturized MIMO antenna for WLAN applications. AEU—Int. J. Electron. Commun. 2021, 136, 153767.
[2] Lin, I.K.C.; Jamaluddin, M.H.; Awang, A.; Selvaraju, R.; Dahri, M.H.; Yen, L.C.; Rahim, H.A. A triple band hybrid MIMO rectangular dielectric resonator antenna for LTE applications. IEEE Access 2019, 7, 122900–122913.
[3] Wu, K.; Cheng, Y.J.; Djerafi, T.; Hong, W. Substrate-integrated millimeter-wave and terahertz antenna technology. Proc. IEEE 2012, 100, 2219–2232. Micromachines 2023, 14, 1284.
[4] Zou, Y.Y.; Kong, Y.D. A Wideband Substrate Integrated Waveguide Slot Antenna with Quad Modes. In Proceedings of the IEEE International Conference on Computational Electromagnetics (ICCEM), Shanghai, China, 20–22 March 2019; pp. 1–3.
[5] Ashraf, N.; Haraz, O.; Ashraf, M.A.; Alshebeili, S. 28/38-GHz dual-band millimeter wave SIW array antenna with EBG structures for 5G applications. In Proceedings of the International Conference on Information and Communication Technology Research (ICTRC), Abu Dhabi, United Arab Emirates, 17–19 May 2015; pp. 5–8.
[6] Cheng, T.; Jiang, W.; Gong, S.; Yu, Y. Broadband SIW cavity-backed modified dumbbell-shaped slot antenna. IEEE Antennas Wirel. Propag. Lett. 2019, 18, 936–940.
[7] Srivastava, A.; Chaudhary, R.K.; Biswas, A.; Akhtar, M.J. Dual-band L-shaped SIW Slot antenna. In Proceedings of the International Conference on Microwave and Photonics (ICMAP), Dhanbad, India, 13–15 December 2013; pp. 6–8.
[8] Petosa, A. Dielectric Resonator Antenna Handbook; Artech House: Norwood, MA, USA, 2007.
[9] Thilagam, B.K.; Kartha, M.M.; Jayakumar, M. Performance Analysis of Cylindrical Dielectric Resonator Antenna with various slot configurations on Substrate Integrated Waveguide. Int. J. Control Theory Appl. 2016, 9, 7581–7588.
[10] Girjashankar, P.R.; Upadhyaya, T. Substrate integrated waveguide fed dual band quad-elements rectangular dielectric resonator MIMO antenna for millimeter wave 5G wireless communication systems. AEU—Int. J. Electron. Commun. 2021, 137, 153821.
[11] Banerjee, S.; Parui, S.K. Bandwidth improvement of substrate integrated waveguide cavity-backed slot antenna with dielectric resonators. Microsyst. Technol. 2020, 26, 1359–1368.
[12] Ashraf, N.; Vettikalladi, H.; Alkanhal, M.A.S. A DR loaded substrate integrated waveguide antenna for 60 GHz high speed wireless communication systems. Int. J. Antennas Propag. 2014, 2014, 146301.
[13] Chemweno, E.K.; Kumar, P.; Afullo, T.J.O. Design of high-gain wideband substrate integrated waveguide dielectric resonator antenna for D-band applications. Optik 2023, 272, 170261.

[14] Iqbal, A.; Tiang, J.J.; Wong, S.K.; Alibakhshikenari, M.; Falcone, F.; Limiti, E. Miniaturization Trends in Substrate Integrated Waveguide (SIW) Filters: A Review. IEEE Access 2020, 8, 223287–223305.
[15] Bilawal, F.; Babaeian, F.; Trinh, K.T.; Karmakar, N.C. The Art of Substrate-Integrated-Waveguide Power Dividers. IEEE Access 2023, 11, 9311–9325.
[16] Kumar, P.; Dwari, S.; Singh, S.; Agrawal, N.K. Design Investigation of a Laminated Waveguide Fed Multi-Band DRA for Military Applications. Frequenz 2018, 72, 7–14.
[17] Kumar, H.; Jadhav, R.; Ranade, S. A Review on Substrate Integrated Waveguide and its Microstrip Interconnect. J. Electron. Commun. Eng. 2012, 3, 36–40.
[18] Lemey, S.; Declercq, F.; Rogier, H. Dual-band substrate integrated waveguide textile antenna with integrated solar harvester. IEEE Antennas Wirel. Propag. Lett. 2014, 13, 269–272.
[19] Kim, S.; Tentzeris, M.M.; Traille, A.; Aubert, H.; Georgiadis, A. A dual-band retrodirective reflector array on paper utilizing Substrate Integrated Waveguide (SIW) and inkjet printing Technologies for Chipless RFID Tag and Sensor Applications. In Proceedings of the IEEE Antennas and Propagation Society International Symposium (APSURSI), Orlando, FL, USA, 7–13 July 2013; pp. 2301–2302.
[20] Cheng, T.; Jiang, W.; Gong, S.; Yu, Y. Broadband SIW cavity-backed modified dumbbell-shaped slot antenna. IEEE Antennas Wirel. Propag. Lett. 2019, 18, 936–940.
[21] Kumar, A.; Bhaskar, S.; Singh, A.K. SIW cavity-backed U-shaped slot antenna for 5G applications. In Proceedings of the IEEE Asia-Pacific Microwave Conference (APMC), Singapore, 10–13 December 2019; pp. 1485–1487. 21. Ta, S.X.; Choo, H.; Park, I. Broadband printed-dipole antenna and its arrays for 5G applications. IEEE Antennas Wirel. Propag. Lett. 2017, 16, 2183–2186.
[22] Srivastava, A.; Chaudhary, R.K.; Biswas, A.; Akhtar, M.J. Dual-band L-shaped SIW Slot antenna. In Proceedings of the International Conference on Microwave and Photonics (ICMAP), Dhanbad, India, 13–15 December 2013; pp. 6–8.
[23] Ashraf, N.; Haraz, O.; Ashraf, M.A.; Alshebeili, S. 28/38-GHz dual-band millimeter wave SIW array antenna with EBG structures for 5G applications. In Proceedings of the International Conference on Information and Communication Technology Research (ICTRC), Abu Dhabi, United Arab Emirates, 17–19 May 2015; pp. 5–8.
[24] Banerjee, S.; Parui, S.K. Bandwidth improvement of substrate integrated waveguide cavity-backed slot antenna with dielectric resonators. Microsyst. Technol. 2020, 26, 1359–1368.
[25] Thilagam, B.K.; Kartha, M.M.; Jayakumar, M. Performance Analysis of Cylindrical Dielectric Resonator Antenna with various slot configurations on Substrate Integrated Waveguide. Int. J. Control Theory Appl. 2016, 9, 7581–7588.
[26] Ashraf, N.; Vettikalladi, H.; Alkanhal, M.A.S. A DR loaded substrate integrated waveguide antenna for 60 GHz high speed wireless communication systems. Int. J. Antennas Propag. 2014, 2014, 146301.
[27] Girjashankar, P.R.; Upadhyaya, T. Substrate integrated waveguide fed dual band quad-elements rectangular dielectric resonator MIMO antenna for millimeter wave 5G wireless communication systems. AEU—Int. J. Electron. Commun. 2021, 137, 153821.
[28] Cheh Lin IK, Jamaluddin MH, Gaya A. A Triple Band Substrate Integrated Waveguide with Dielectric Resonator Antenna for 4G and 5G Applications. Micromachines. 2023; 14(7):1284.